HYPERSPECTRAL ESTIMATION OF FOXTAIL MILLET (*SETARIA ITALICA*) GRAIN PROTEIN CONTENTS BY USING PHOTOSYNTHETIC RATE PARAMETERS UNDER DIFFERENT PHOTOPERIODS

LI, H. Y.[1] – LI, R.[1] –TIAN, X.[2] – CHEN, L.[2] – WANG, H. G.[2] – FAHAD, S.[3] – QIAO, Z. J.[2*] – WANG, J. J.[2*]

[1]*College of Agriculture, Shanxi Agricultural University, Taigu, China (phone: +86-189-3949-9172)*

[2]*Center for Agricultural Genetic Resources Research, Shanxi Agricultural University, Taiyuan, China*

[3]*Institute of Molecular Biology and Biotechnology, The University of Lahore, Lahore, Pakistan*

**Corresponding author*
e-mail: xiaoleiwangjie@163.com; phone: +86-152-3404-0919
nkypzs@126.com; phone: +86-139-3422-3541

(Received 2nd Nov 2023; accepted 4th Mar 2024)

Abstract. To predict the grain protein content of foxtail millet in a timely, effective, and rapid manner, the study used the net photosynthetic rate of leaves as an intermediate parameter. By using hyperspectral reflectance-net photosynthetic rate of leaves-grain protein content and using the 2020 potted plant experiment data, hyperspectral data and its first derivative (1ST) data with different photoperiod treatments, the models were constructed using machine learning algorithms (SVM, PLS and BP) based on net photosynthetic rate. The results revealed that the accuracy of the SVM model was better than that of the PLS model and BP model, and the SVM model based on the first derivative (1ST) spectral reflectivity was better than the original spectral (R) reflectivity, the R^2, RMSE, RPD of the modeling set and validation set were 0.988, 0.732, 0.823, 4.061, 8.697, 1.810, respectively The correlation coefficient between net photosynthetic rate and grain protein content was 0.872 and R^2 was 0.719 at 10 days after anthesis. The SVM model can be used to accurately monitor the grain protein content of foxtail millet, and provide technical support for hyperspectral techniques in high-yield cultivation and Intensive farming of foxtail millet.
Keywords: *photoperiod, SVM model, foxtail millet, grain protein content, canopy spectral reflectance*

Introduction

Hyperspectral remote sensing offers high spectral resolution, and strong band continuity and can provide fine spectral information which is useful (Tian et al., 2018). In recent years, the research on hyperspectral technology has become more extensive and its usage in the determination of crop growth and quality has increased. Foxtail millet (*Setaria italica*) is a short-day crop which requires adequate light during the whole growth and produces nutritious grains (Tian et al., 2021). Previous studies have reported that grain proteins can be analyzed by using hyperspectral reflectance. In this context, Zhang et al. (2015) used partial least squares (PLS) to establish a reliable model for rapid and nondestructive estimation of soluble protein content in rape leaves. Similarly, Sonobe Rei et al. (2020) established a prediction model of chlorophyll content in tea based on kernel-based extreme learning machine (KELM). Zhao et al. (2020) analyzed the canopy spectra of 122 representative quinoa cultivars and used

http://www.aloki.hu ● ISSN 1589 1623 (Print) ● ISSN 1785 0037 (Online)
DOI: http://dx.doi.org/10.15666/aeer/2202_16671682

partial least squares (PLS) to construct a quantitative prediction model of Quinoa Wheatberry crude protein content. In another study, near-infrared spectroscopy was used to establish a least squares model for the prediction of starch, amylose, and proteins (Tian et al., 2021). Similarly, Hyperspectral imaging combined with machine learning algorithms can rapidly and non-destructively predict the protein and fat contents of sorghum (Fei et al.,2023). The improved partial least squares (MPLS) model exhibited better accuracy in predicting oat grain protein contents using spectral techniques (Qiao et al., 2016). Moreover, Zhang et al. (2018) found that the SVM model based on the feature bands extracted by the continuous projection algorithm (SPA) could predict the protein content of the winter Support vector machine. Lastly, Guo et al. (2023) established a prediction model for corn grain yield based on hyperspectral data.

Summarizing this information, a few reports relate the influence of photoperiod on foxtail millet grain physiology by using spectroscopy. To predict the grain protein content of foxtail millet in a timely, effective, and rapid manner. This study utilized various machine learning algorithms viz. partial least square (PLS) (Gaydou et al., 2011), support vector machine (SVM) (Vohland et al., 2011), and backpropagation (BP) to accurately predict the grain protein contents. Initially, the prediction model of the net photosynthetic rate of foxtail millet leaves under different photoperiod treatments was established. Later on, the prediction model of grain protein content was established by using leaf net photosynthetic rate as an intermediate agronomic parameter to provide technical support for rapid and accurate acquisition of foxtail millet growth and grain quality information.

Materials and methods

Experimental conditions

The pot trial was conducted in 2020 at Dingxiang fine seed farm, Xinzhou (38.4167° N, 112.7342° E), China, and the foxtail millet variety named Zhangzagu 10 was investigated. The pelvic floor radius was 10 cm, the pelvic mouth radius was 15 cm, the height was 25 cm, and the volume was 12435 cm^3. The environmental conditions suitable for the growth of foxtail millet were the followings: annual rainfall was 430 mm, an annual mean air temperature was 8.7°C, a frost-free period is about 157 days, an annual sunshine duration was 2734.5 h. The composition of potting soil is the same as that of field soil, which uses 0~20 cm field soil to grow foxtail millet. Total nitrogen (0.82 $g \cdot kg^{-1}$), available phosphorus (17.3 $mg \cdot kg^{-1}$), available potassium (93 $mg \cdot kg^{-1}$), organic matter (12.5 $g \cdot kg^{-1}$), pH (8.16) and the soil water contents were recorded.

Experimental design

Briefly, twenty seeds were planted in each pot and five pots were planted for each treatment. Afterward, ten seedlings with the same growth potential were selected from each pot with eight light treatments (*Table 1*). Photoperiod treatments were carried out from the three-leaf stage to the mature stages. Among them, the length of the short-day treatment was set to 12 h (from 19:00 p.m. to 7:00 am the next day for shading treatment, other times without shading treatment). The canopy spectral reflectance and net photosynthetic rate of foxtail millet were measured at the beginning of the anthesis every 10 days after the anthesis and at the mid-filling stage for 50 days. Each pot was tested once, a total of 5 times, and average values were used for data analyses. The net

http://www.aloki.hu ● ISSN 1589 1623 (Print) ● ISSN 1785 0037 (Online)
DOI: http://dx.doi.org/10.15666/aeer/2202_16671682

photosynthetic rate of the parietal leaves of the same plant was measured immediately after each measurement of spectral data. No fertilizer was applied during the period of foxtail millet growth. The relative water content of the soil was determined at 6 h each afternoon using a soil moisture meter to maintain the water content at 60%. Reduction rates that do not use full shading or quantitative lighting.

Table 1. *Different photoperiod treatments in the experiment*

Dispose	Trilobar - Jointing	Jointing – Flowering	Flowering - Maturity
CK	Natural Sunshine	Natural Sunshine	Natural Sunshine
G1	Natural Sunshine	Short Sunshine	Natural Sunshine
G2	Natural Sunshine	Natural Sunshine	Short Sunshine
G3	Natural Sunshine	Short Sunshine	Short Sunshine
G4	Short Sunshine	Short Sunshine	Natural Sunshine
G5	Short Sunshine	Natural Sunshine	Short Sunshine
G6	Short Sunshine	Short Sunshine	Short Sunshine
G7	Short Sunshine	Natural Sunshine	Natural Sunshine

Determination of spectral reflectance and eco-physiological indices

Canopy spectrum

The FieldSpec 4 portable spectrometer (US company Analytical Spectral Device, ASD) was used to record the spectral parameters (*Fig. 1*). The spectral sampling interval of 350-1000 nm was 1.4 nm with the following parameters: spectral resolution of 3 nm; 1000-2500 nm spectral sampling interval of 2 nm, and spectral resolution of 10 nm. The measurements of the foxtail millet canopy spectrum were carried out from 10:00 am-14:00 pm under clear weather, with no wind or very small wind speed (The wind speed is less than 3 m/s). During measurement, the standard whiteboard correction was carried out in time before and after the observation of each group of targets.

Figure 1. *The FieldSpec 4 portable spectrometer*

http://www.aloki.hu ● ISSN 1589 1623 (Print) ● ISSN 1785 0037 (Online)
DOI: http://dx.doi.org/10.15666/aeer/2202_16671682

Determination of grain weight per plant

Grain weight per plant (GWP,g) was recorded at harvest.

Determination of starch content in grain

The soluble sugars and starch were separated by 80% ethanol, and the starch was further hydrolyzed to glucose by acid hydrolysis. The glucose content was determined at 560 nm with an anthrone reagent on a SP-756P UV-Vis spectrophotometer (Shanghai Spectral Co., Ltd.).

Determination of net photosynthetic rate in leaves and protein content in grains

At the same time, the net photosynthetic rate of the same plant was measured by CI -340 portable photosynthetic apparatus (US CID Bio-Science) (*Fig. 2*). Moreover, the nitrogen contents from the grains were recorded by the Kjeldahl nitrogen analyzer and calculated as follows:

$$\text{Grain protein content (GPC,\%)} = 6.25 \times \text{Grain nitrogen content}$$

Figure 2. *CI -340 portable photosynthetic apparatus*

Derivation and validation of statistical models

The values of net photosynthetic rate measured in different periods were sorted from low to high, and the net photosynthetic rate and corresponding spectral reflectance were divided into modeling sets and verification sets according to 3:1 by concentration gradient method. Using the continuous projection algorithm (SPA) to determine the characteristic bands the models were constructed using Partial least squares regression (PLS), Support vector machine (SVM), and Back Propagation (BP) neural networks. Each model was evaluated by coefficient of determination (R^2), root mean squared error (RMSE), and Residual prediction difference (RPD), the closer the R^2 is to 1, the smaller the RMSE, indicating that the prediction accuracy of the model is better. When the RPD is greater than 2, the prediction precision of the model is good. When the RPD is greater than 1.4, the model has medium prediction precision. When the RPD is less than 1.4, the prediction precision of the model is poor. The formula is as follows:

http://www.aloki.hu ● ISSN 1589 1623 (Print) ● ISSN 1785 0037 (Online)
DOI: http://dx.doi.org/10.15666/aeer/2202_16671682

$$R^2 = \frac{\sum_{i=1}^{n}(Y_i' - \bar{Y}_i)^2}{\sum_{i=1}^{n}(Y_i - \bar{Y}_i)^2} \quad \text{(Eq.1)}$$

$$RMSE = \sqrt{\frac{1}{n}\sum_{i=1}^{n}\left(Y_i - Y_i'\right)^2} \quad \text{(Eq.2)}$$

$$\text{RPD} = \frac{\text{SD}}{\text{RMSE}} \quad \text{(Eq.3)}$$

$$SD = \sqrt{\frac{\sum(Y_i - \bar{Y}_i)^2}{n-1}} \quad \text{(Eq.4)}$$

In the formula, n is the number of samples; Y'_i indicates the predicted value of the sample; Y_i represents the measured value of the sample; $\bar{Y}_i$ represents the average of the measured values; RMSE denotes root mean square error; SD represents the standard deviation of the measured sample.

Statistical analyses

The data were analyzed by IBM SPSS Statistics 26.0; Using MATLAB2010A to extract the SPA feature band, and build PLS and SVM model. Using Matlab 2018A to build the BP neural network model; Unscrambler 9.7 was used to perform the first-order differential processing of the spectral data; Origin 2021 and Excel 2019 were used for the mapping analysis.

The formula for calculating the first-order differential spectra is as follows:

$$R'(\lambda_i) = \frac{dR\lambda_i}{d\lambda} = \frac{R(\lambda_{i+1}) - R(\lambda_{i-1})}{2\Delta\lambda} \quad \text{(Eq.5)}$$

In the formula, λ_i is the wavelength of each band, $R\lambda_i$ is the original spectral reflectivity corresponding to band i ; $R'(\lambda_i)$ is the first-order differential spectrum at ban i ; $\Delta\lambda$ is the interval between the wavelength λ_{i-1} and λ_i, the apparent spectral sampling interval is determined.

Results

Effects of different photoperiod treatments on net photosynthetic rate (PN), grain protein content (GPC), grain starch content (GSC) and grain weight per plant (GWP)

The net photosynthetic rate of CK, G1, and G3 reached a peak at the middle of filling stage and the net photosynthetic rate of other treatments reached a peak at 10 d after anthesis (*Fig. 3*). Therefore, short-day treatment before the jointing stage can accelerate the growth process of foxtail millet. The difference in net photosynthetic rate between G6 and CK was significant before 40 d after anthesis, the net photosynthetic rate of G6 was significantly higher than that of CK. The net photosynthetic rates of G7 and CK were significantly different at anthesis, 10 d after anthesis, the middle of filling stage, and 30 d after anthesis, the net photosynthetic rate of G7 was significantly higher than that of CK at anthesis, 10 d after anthesis, and 30 d after anthesis, and significantly lower than that of CK at the middle of filling stage; There was significant difference between G4 and G1 at anthesis, 10 d after anthesis and the middle of filling stage. The

http://www.aloki.hu ● ISSN 1589 1623 (Print) ● ISSN 1785 0037 (Online)
DOI: http://dx.doi.org/10.15666/aeer/2202_16671682

net photosynthetic rate of G4 was significantly higher than that of G1; G2 and CK were significantly different only at 10 d and 20 d after anthesis, the net photosynthetic rate of G2 was significantly higher than that of CK; The net photosynthetic rate of G5 was significantly higher than that of G7 at the middle of filling stage and 20 days after anthesis. Short-day treatment of foxtail millet from the three-leaf stage to the jointing stage can significantly increase the net photosynthetic rate of foxtail millet from the flowering period to the middle of filling stage.

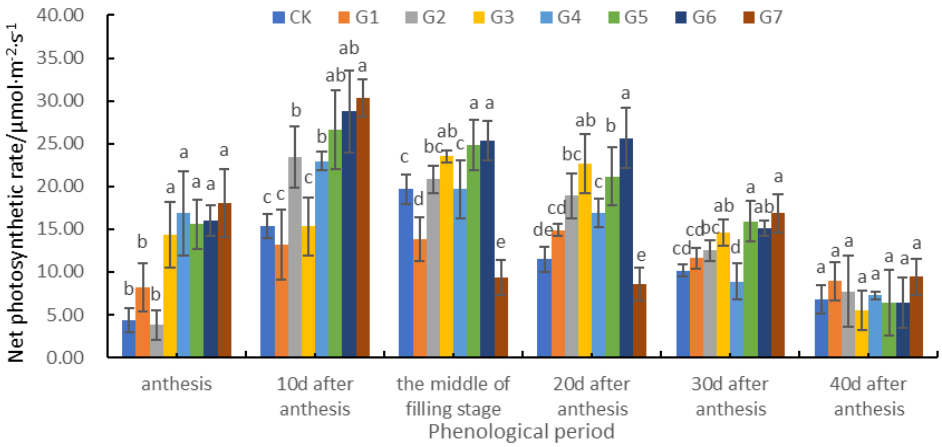

Figure 3. *Effect of different photoperiod treatments on net photosynthetic rate (Pn). LSD multiple comparisons and Duncan's test were used to test the significance of differences, and error bars indicate standard errors*

The grain protein content of G6 increased by 2.52% compared with CK (*Fig. 4*). In all treatments, the protein content of G7 seeds was the highest (12.1%), the protein content of G1 grain was the lowest (9.42%), There was no significant difference in grain protein content between G1 and CK, the difference was only 0.07%. The difference in grain protein content between G6 and G7 was not significant, only 0.14%.

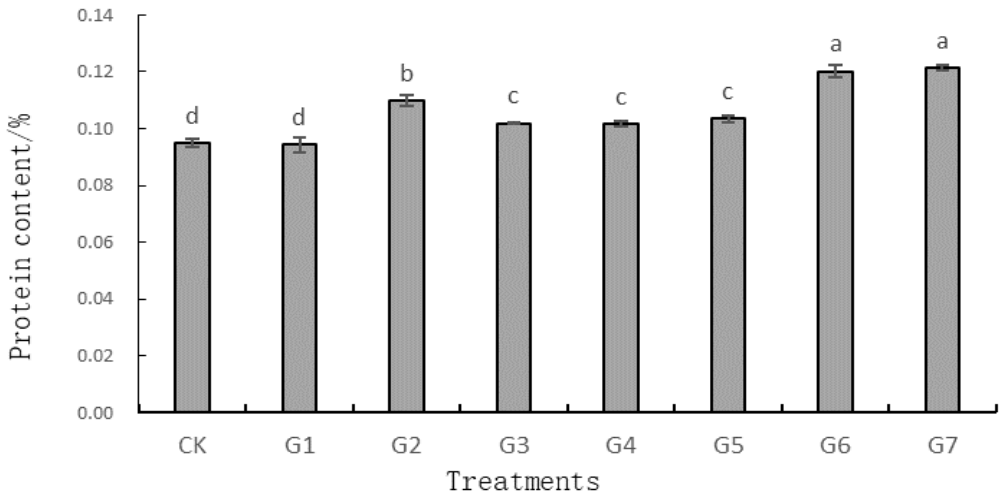

Figure 4. *Effects of different photoperiod treatments on grain protein content (GPC). LSD multiple comparisons and Duncan's test were used to test the significance of differences, and error bars indicate standard errors*

http://www.aloki.hu ● ISSN 1589 1623 (Print) ● ISSN 1785 0037 (Online)
DOI: http://dx.doi.org/10.15666/aeer/2202_16671682

Short-day treatment (G2) from flowering to maturity could significantly reduce grain starch content in foxtail millet, G2 decreased by 7.35% compared with CK; Compared with CK, G5 decreased significantly by 3.46%; G3 and G7 were significantly higher than CK, G3 increased by 2.18% and G7 increased by 2.96% compared with CK (*Fig. 5*).

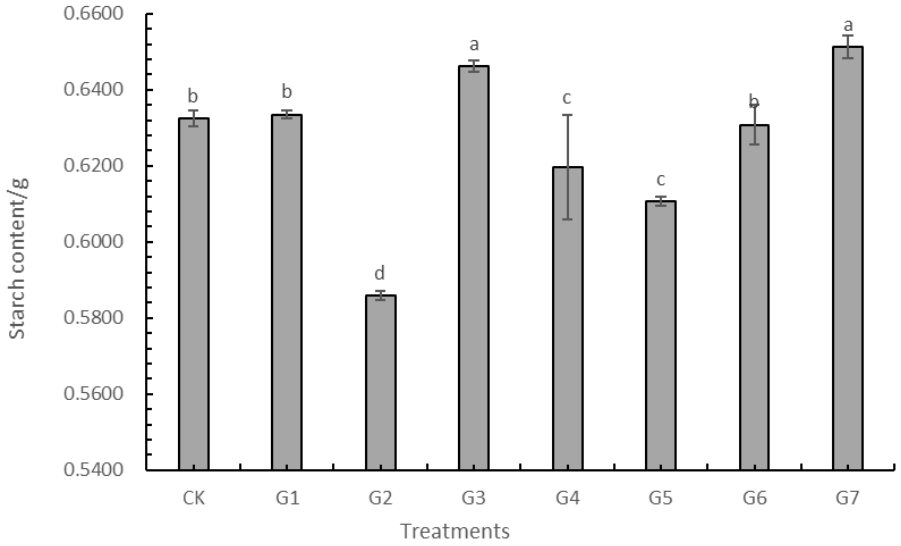

Figure 5. *effect of different photoperiod treatments on grain starch content (GSC). LSD multiple comparisons and Duncan's test were used to test the significance of differences, and error bars indicate standard errors*

Grain weight per plant is one of the main indexes for high yield of foxtail millet. G3 had the highest grain weight per plant, which was 5.45 g, Compared with CK, CK increased by 0.94 g and increased by 20.8% (*Fig. 6*). The other treatments had no significant difference with CK. The results indicated that short-day treatment after jointing stage could significantly increase grain weight per plant of foxtail millet.

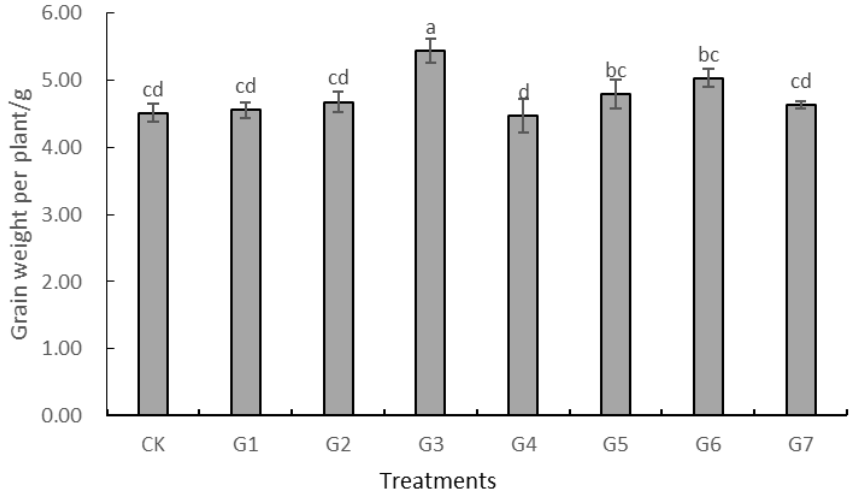

Figure 6. *Effects of different photoperiod treatments on grain weight per plant (GWP). LSD multiple comparisons and Duncan's test were used to test the significance of differences, and error bars indicate standard errors*

http://www.aloki.hu ● ISSN 1589 1623 (Print) ● ISSN 1785 0037 (Online)
DOI: http://dx.doi.org/10.15666/aeer/2202_16671682

Spectral characteristic analysis

The canopy spectral reflectance of foxtail millet at different phenological stages was different, but the trend was similar. There is a reflection peak at about 555 nm due to the poor absorption of green light by photosynthetic pigments. Because the red light is absorbed by chlorophyll, there is an absorption valley at the wavelength of 675 nm. Between 680 and 760 nm, the spectral reflectivity increases rapidly. There is an absorption valley at 955 nm and a reflection peak at 1660 nm. To reduce the noise impact, data at 1800-1950 nm and 2450-2500 nm were excluded for analysis, and significant differences were found in the near-infrared light band (*Fig. 7*).

In the visible region, the reflectivity of 40 d after anthesis is the largest, followed by 30 d after anthesis, anthesis,10 d after anthesis, 20 d after anthesis. The reflectivity of 20 d after anthesis is the smallest; At 780-930 nm, the reflectivity of the six periods is 30 d after anthesis, anthesis,20 d after anthesis,40 d after anthesis,10 d after anthesis, the middle of filling stage; After 930 nm, the reflectivity of 30 d after anthesis was the highest, followed by 40 d after anthesis, before 1360 nm, the smallest was the middle of filling stage, and after 1400 nm, the smallest was 20 d after anthesis.

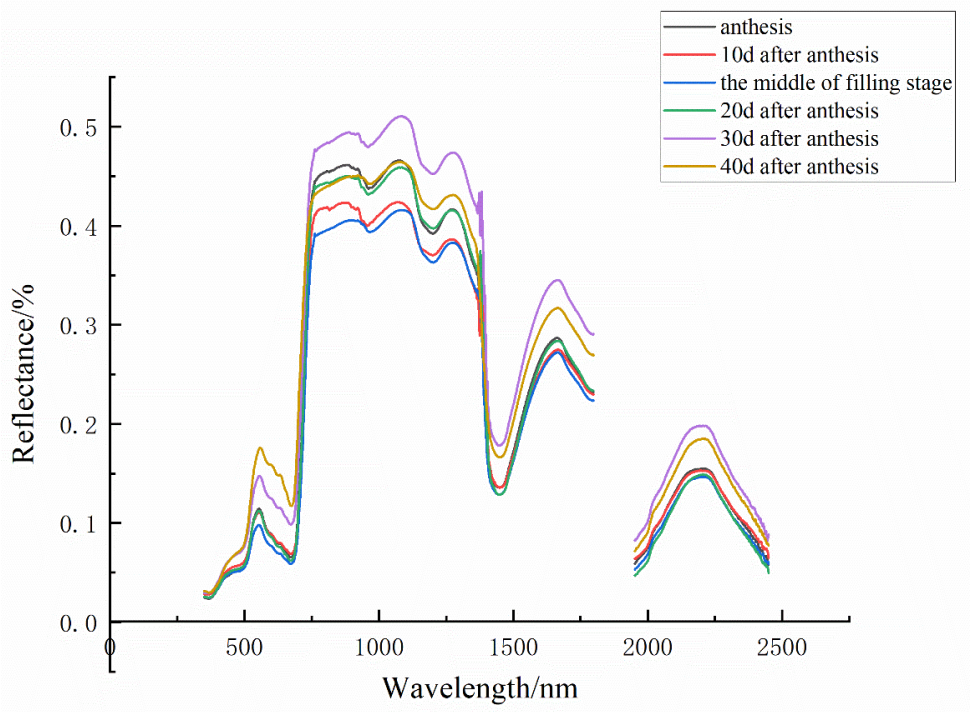

Figure 7. *Spectral reflectance of the foxtail millet canopy*

Correlation analysis between leaf net photosynthetic rate (PN) and hyperspectral data and establishment of characteristic band

The sensitive bands of leaf net photosynthetic rate were mainly concentrated between 460-740 nm and 1400-1800 nm (*Fig. 8*). In the first derivative spectral reflectance, the sensitive band of net photosynthetic rate is mainly concentrated in 500-800 nm. According to the continuous projection algorithm (SPA) analysis, the characteristic bands of net photosynthetic rate were determined as 710, 1920, 1881, and 1865 nm. The characteristic bands of the first derivative were 486, 1873, 2188, and 1835 nm.

http://www.aloki.hu ● ISSN 1589 1623 (Print) ● ISSN 1785 0037 (Online)
DOI: http://dx.doi.org/10.15666/aeer/2202_16671682

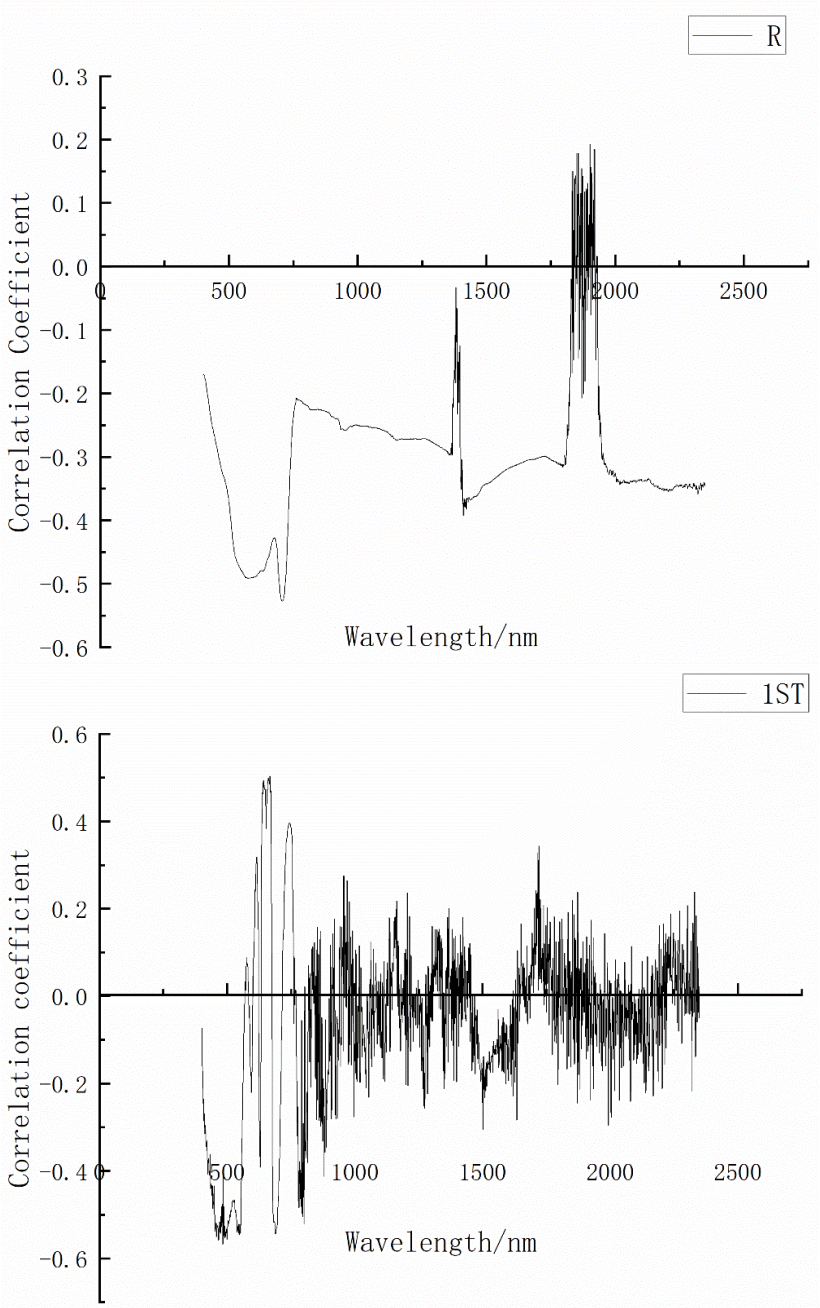

Figure 8. *Correlation of leaf net photosynthetic rate (Pn) with canopy spectral reflectance and first-derivative spectral reflectance*

Hyperspectral model of leaf net photosynthetic rate (PN)

The R^2 of all the model sets is greater than 0.600, which shows that the model accuracy of the model sets was better (*Table 2*). The R^2 of the 1ST-SVM model sets was 0.988 and the RMSE was 0.823, and the RPD was 8.288 which was better than other models. Among all the models in the verification set, the verification set R^2 of 1ST-SVM was 0.732, the RMSE was 4.061, and the RPD was 1.810 which indicated that the model has moderate prediction ability and the precision was best compared with other models. The accuracy of all models based on the characteristic band was much

http://www.aloki.hu ● ISSN 1589 1623 (Print) ● ISSN 1785 0037 (Online)
DOI: http://dx.doi.org/10.15666/aeer/2202_16671682

lower than that based on the full-band data, and the actual and predicted values of leaf net photosynthetic rate were 1:1 when different models were used to predict leaf net photosynthetic rate (*Fig. 9.*), it can be seen that 1ST-SVM Model R^2 is the largest, 0.915, RMSE is the smallest, 2.152, RPD is the largest, 3.338, which is consistent with the above results.

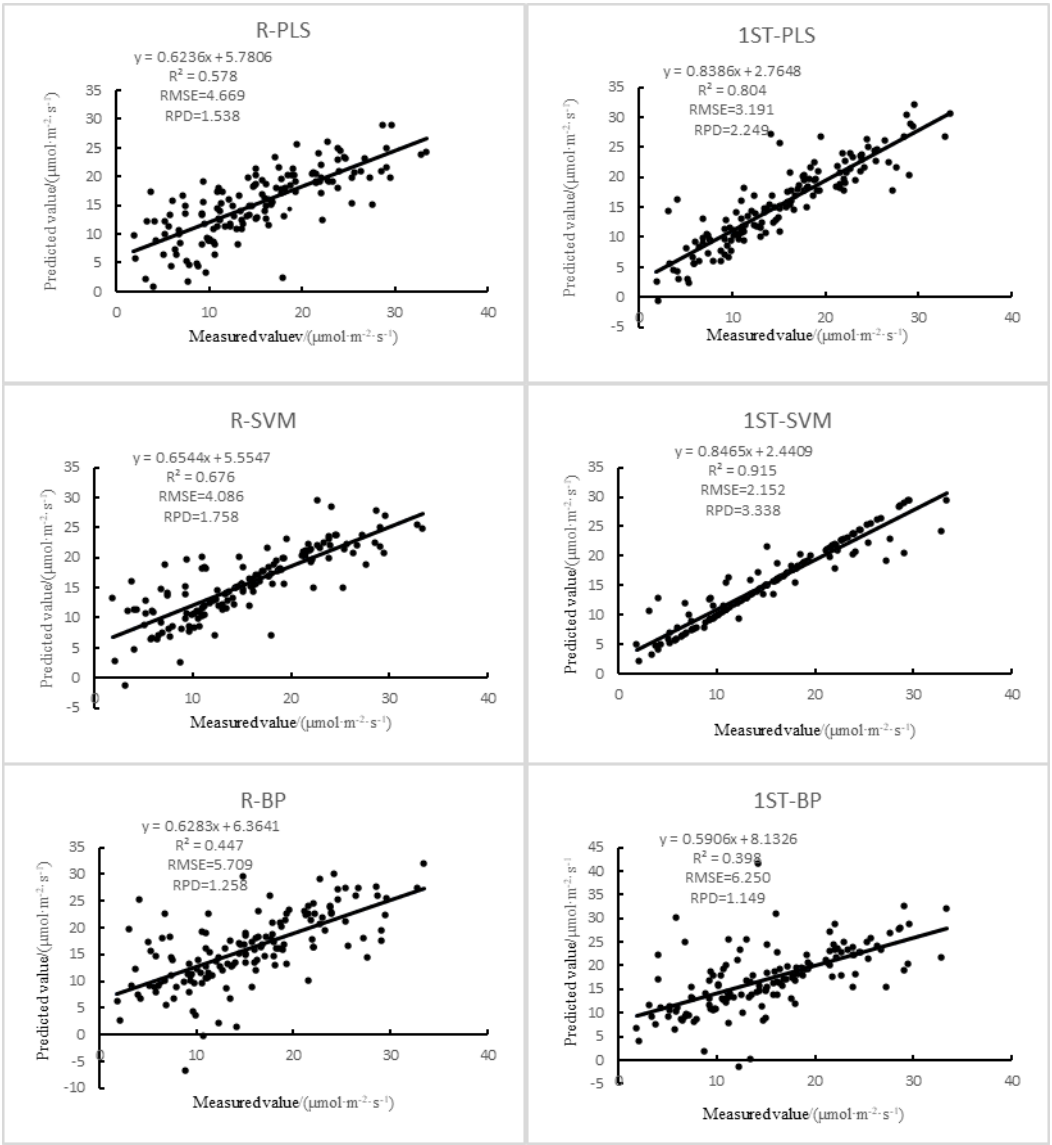

Figure 9. *Comparison of measured and predicted net photosynthetic rates for different models*

Establishment of spectral model of grain protein content (GPC) based on leaf net photosynthetic rate (PN)

The correlation between the net photosynthetic rate of leaves and grain protein content was analyzed. It can be seen from *Table 3* that the net photosynthetic rate of leaves measured by 10 d after anthesis showed a very significant positive correlation with grain protein content, therefore, a monitoring model for predicting grain protein content based on leaf net photosynthetic rate can be established.

http://www.aloki.hu ● ISSN 1589 1623 (Print) ● ISSN 1785 0037 (Online)
DOI: http://dx.doi.org/10.15666/aeer/2202_16671682

Table 2. *Fitting (n = 108) and validation (n = 36) of the foxtail millet leaf net photosynthetic rate (Pn) and hyperspectral data model*

Model type	Modeling set			Validation set		
	R^2	RMSE	RPD	R^2	RMSE	RPD
R-PLS	0.630	4.335	1.652	0.459	5.551	1.324
1ST-PLS	0.926	1.936	3.669	0.484	5.436	1.352
R-SVM	0.744	3.713	1.929	0.558	5.044	1.457
1ST-SVM	0.988	0.823	8.697	0.732	4.061	1.810
R-BP	0.627	4.426	1.618	0.150	8.462	0.869
1ST-BP	0.625	4.760	1.504	0.101	9.396	0.782
R-PLS(SPA)	0.284	6.033	1.187	0.485	5.557	1.323
1ST-PLS(SPA)	0.329	5.839	1.226	0.504	5.267	1.396
R-SVM(SPA)	0.340	5.863	1.187	0.540	5.123	1.323
1ST-SVM(SPA)	0.326	5.893	1.215	0.647	4.978	1.477
R-BP(SPA)	0.283	6.052	1.183	0.455	5.479	1.341
1ST-BP(SPA)	0.333	5.823	1.230	0.265	6.289	1.169

Table 3. *Correlation between leaf net photosynthetic rate and protein content at different phenophases*

	Anthesis	10 d after anthesis	The middle of filling stage	20 d after anthesis	30 d after anthesis	40 d after anthesis
GPC (%)	0.492	0.872**	-0.090	0.126	0.665	0.183

** and * indicate significant correlations at 0.05 and 0.01 levels, respectively

The fitting equation between the net photosynthetic rate of leaves and grain protein content was established by using flowering time and different days after anthesis (*Table 4*). The equation reflects the quantitative relationship between the net photosynthetic rate of leaves and grain protein content. The determination coefficients were 0.334, 0.719, 0.415, 0.405, 0.349 and -0.278 respectively. The determination coefficient of net photosynthetic rate and grain protein content of 10 d after anthesis was the highest, R^2 was 0.719, 40 d after anthesis is the lowest and negative value, which shows that the model is extremely unreliable. Therefore, the hyperspectral prediction model of grain protein can be established by using the leaf net photosynthetic rate 10 d after anthesis as the link point, this is consistent with the correlation analysis between net photosynthetic rate of leaves and grain protein content.

Table 4. *Model of net photosynthetic rate and grain protein content of leaves at different periods after flowering of the foxtail millet*

	Fit the equation	R^2
Anthesis	$Y = 0.1226 - 0.0062 * x + 0.0003 * x^2$	0.334
10 d after anthesis	$Y = 0.0758 + 0.0014 * x$	0.719
The middle of filling stage	$Y = 0.1927 - 0.0108 * x + 0.0003 * x^2$	0.415
20 d after anthesis	$Y = 0.1711 - 0.0088 * x + 0.0003 * x^2$	0.405
30 d after anthesis	$Y = 0.0738 + 0.0024 * x$	0.349
40 d after anthesis	$Y = 0.1824 - 0.0222 * x + 0.0016 * x^2$	-0.278

http://www.aloki.hu ● ISSN 1589 1623 (Print) ● ISSN 1785 0037 (Online)
DOI: http://dx.doi.org/10.15666/aeer/2202_16671682

Discussion

Effects of photoperiod on grain protein content, grain starch content, and grain weight per plant in foxtail millet

The results showed that short-day treatment before the jointing stage could significantly accelerate the growth of foxtail millet and increase the protein content of foxtail millet grain but could decrease the grain weight per plant; It was concluded that the photoperiod sensitive period was from the seedling stage to the jointing stage, and short-day treatment after jointing stage had little effect on the growth process of foxtail millet. This is because foxtail millet is a short-day crop, short-day treatment can accelerate its growth process so that foxtail millet flowering ripens ahead of time. Li et al. (2024) found that the total nitrogen content of cucumber seedlings showed a significant decreasing trend with the increase of photope. Wang et al. (2021) found that photoperiod could significantly affect the growth and development process of broomcorn foxtail millet and its growth hormone content, and that long sunshine could significantly delay the growth period of broomcorn foxtail millet and increase the net photosynthetic rate of broomcorn foxtail millet leaves, but it will reduce the protein content of the foxtail millet grain. This is consistent with the results of this study. The protein content of foxtail millet is usually between 9.2% and 14.7%, the grain protein content of foxtail millet was 9.485% under natural light during the whole growth period, and 12.0% of the total growth period under short sunshine, the results showed that short sunshine could significantly increase grain protein content of foxtail millet. Yang et al. (2017) found that foxtail millet yield decreased under low light stress at the jointing stage. Wang (2022) found that maize yield decreased under low light stress, which is consistent with the results of this experiment.

The effect of short-day treatment on grain starch content was different from that of grain protein content and grain weight per plant, under the treatment of natural light from the trifoliate stage to the jointing stage, the reduction of starch content in grains under short sunshine after anthesis stage was significantly higher than that under short sunshine from jointing stage to anthesis stage. This is due to the reproductive growth stage of the plant after flowering, short-day treatment to shorten the time of photosynthesis, thus reducing the accumulation of organic products, resulting in a reduction in grain starch content. Under the treatment of short sunlight from the trifoliate stage to the jointing stage, the increase of starch content in grains under natural light after the anthesis stage was significantly higher than that under natural light from the jointing stage to the anthesis stage, and the starch content of grain in jointing stage-maturity stage under natural light treatment was higher than that in other treatments. It was found that the starch content increased significantly by prolonging the illumination time. Chen et al. (2017) used duckweed as a material to study the effects of different photoperiods on the accumulation of duckweed starch through different dark period treatments. The results showed that the longer the illumination time was, the better the effect of starch accumulation was. By setting different photoperiods before and after the flowering period, Shen et al. (2015) studied the effects of photoperiod on growth and development, yield, and nutritional quality of wheat. The results showed that prolonged photoperiod could increase the starch content in grains, which was consistent with the experimental results.

Hyperspectral monitoring of net photosynthetic rate in foxtail millet leaves

Photosynthesis is the process by which plant leaves absorb and convert light energy and is the basis to produce matter (Wang et al., 2020), light duration is one of the main

http://www.aloki.hu ● ISSN 1589 1623 (Print) ● ISSN 1785 0037 (Online)
DOI: http://dx.doi.org/10.15666/aeer/2202_16671682

factors affecting the accumulation of photosynthetic products. Ran et al. (2017) research found that night light supplementation can improve the hormone content and light efficiency of wheat, promote grain filling and increase yield. This is different from the results of this study. In this study, it was found that the net photosynthetic rate of foxtail millet could be increased by short-day treatment before the jointing stage, which may be due to the shortened growth process of foxtail millet, as a result, the foxtail millet treated with short sunlight had earlier growth period than the foxtail millet treated with natural light. Therefore, the net photosynthetic rate of foxtail millet treated with short sunlight was not consistent with that of foxtail millet treated with natural light. The accuracy of the rice net photosynthetic rate prediction model established by Liu et al. (2016) using support vector machine (SVM) was above 83%. The results showed that the nu-SVR-linear grid search model had the best generalization ability. This is consistent with the results of this study. This is because SVM algorithm is based on nonlinear mapping theory, using kernel function instead of high-dimensional space mapping, has less robustness, and can maximize the prediction accuracy in the case of small samples, compared with PLS algorithm and BP neural network, it has stronger generalization ability. The results of this study show that: The accuracy of 1ST-SVM model is the best 10 d after flowering, and the R^2, RMSE and RPD of hyperspectral model based on leaf net photosynthetic rate were 0.988, 0.823 and 8.697, respectively, the validation set has an R^2 of 0.732, an RMSE of 4.061, and an RPD of 1.810.

Hyperspectral monitoring of grain protein content in foxtail millet

More than 90% of plant dry matter comes from the photosynthetic carbon fixation reaction (Sheng et al., 2022.), and crops change from vegetative growth to reproductive growth after flowering, so photosynthetic characteristics are closely related to grain protein content. At present, there are two main methods to monitor grain protein by spectral technique, one is the direct method (spectral data-grain protein content) (Gao et al., 2019; Zhang et al., 2023; Singh et al., 2023.), and one is indirect (spectral information-intermediate parameters-grain protein content) (Li et al.2018.). Based on the idea of “Spectral information-net photosynthetic rate in leaves-protein content in grains” (Han et al.2018.), the agronomic correlation between net photosynthetic rate and organic matter content in crops was studied, combined with previous studies (Miao et al., 2020; Liu et al., 2020; Lv et al., 2017), the net photosynthetic rate of leaves was determined as the connecting point, and the prediction model of grain protein content after flowering was constructed. The fitting equation of net photosynthetic rate and grain protein content in 10 days after anthesis was 0.719, the results showed that the hyperspectral 1ST-SVM model based on the net photosynthetic rate of foxtail millet leaves at the grain filling stage was effective in predicting grain protein content of foxtail millet. He et al. (2017) used Partial least squares regression (PLS) to develop a prediction model for the protein content of winter wheat at maturity, with an R^2 of 0.979 based on the grain filling stage. Wang et al. (2019) constructed a model for monitoring the protein content of the foxtail millet grain, and the model based on different growth stages was optimized for the grain-filling stage, with R^2 being 0.798. This is consistent with the results of this experiment; this is because the accumulation of protein in grains is not linear. Before anthesis, it is mainly vegetative growth, and the accumulation of protein is slow. After anthesis and filling, the accumulation of protein is mainly reproductive growth, and the accumulation of protein is accelerated, so the precision of the model is the highest in the grouting period. Qu et al. (2017) found that the model for

http://www.aloki.hu ● ISSN 1589 1623 (Print) ● ISSN 1785 0037 (Online)
DOI: http://dx.doi.org/10.15666/aeer/2202_16671682

predicting grain protein content based on plant nitrogen content at the anthesis stage of winter wheat had the best precision, there are some differences between the results and this experiment, which may be caused by the different crops and their physiological habits.

There are still some deficiencies in this study. When foxtail millet grows to a certain extent, its roots will be affected by external high temperatures and other environments and may have some differences compared with field experiments. In the study, the main promoted variety Zhangzagu 10 was used as the research material, so the model was suitable for the planting area of spring seeding foxtail millet varieties in Shanxi Province. In addition, this experiment only considered 12 h of short-day sunshine and did not design other conditions for short-day and long-day sunshine. Therefore, the next step is to make a comprehensive analysis of the light time and model correction to establish a set of multi-factor prediction models of grain protein.

Conclusions

We conclude that the net photosynthetic rate of foxtail millet increased significantly from flowering to the middle of filling stage by short-day treatment, in addition, short-day treatment could significantly increase the grain protein content of foxtail millet, but decrease the grain weight per plant, a 1ST-SVM model was constructed to predict grain protein content of foxtail millet, in which 1ST-SVM model based on net photosynthetic rate 10 days after anthesis could accurately predict grain protein content, this study is helpful to optimize field management and grain quality grading of foxtail millet, and provide theoretical basis for rapid and accurate acquisition of foxtail millet growth information and grain quality.

Acknowledgements. This work was supported by Graduate Education Reform and Quality Improvement Program of College of Agriculture, Shanxi Agricultural University (2023YCX50), Ministry of Finance and Ministry of Agriculture and rural areas (CARS-06-14.5-A16), Technological Innovation and Upgrading Project, Shanxi Agricultural University (CXGC2023038).

REFERENCES

[1] Chen, X. Y., Yang, Q. Y., Zhao, Q. (2017): Effect of different photoperiod on the growth and starch accumulation of duckweed. – Northern Horticulture (22): 50-54.
[2] Fei, X., Jiang, X. N., Lei, Y., Tian, J. P., Hu, X. J., Bu, Y. H., Huang, D., Luo, H. B. (2023): The rapid non-destructive detection of the protein and fat contents of sorghum based on hyperspectral imaging. – Food Analytical Methods 16(11-12): 1690-1701.
[3] Gao, R., Li, Z. D., Ma, Z., Kong, Q. M., Muhammad Rizwan, Su, Z. B. (2019): Research on crude protein of pasture based on hyperspectral imaging. – Spectroscopy and Spectral Analysis 39(10): 3245-3250.
[4] Gaydou, V., Kister, J., Dupuy, N. (2011): Evaluation of multiblock NIR/MIR PLS predictive models to detect adulteration of diesel/biodiesel blends by vegetal oil. – Chemometrics and Intelligent Laboratory Systems 106(2): 190-197.
[5] Guo, Y. H., Xiao, Y., Hao, F. H., Zhang, X., Chen, J. H., de Beurs Kirsten, He, Y. H., Fu, Y. H. (2023): Comparison of different machine learning algorithms for predicting maize grain yield using UAV-based hyperspectral images. – International Journal of Applied Earth Observation and Geoinformation 124.

http://www.aloki.hu ● ISSN 1589 1623 (Print) ● ISSN 1785 0037 (Online)
DOI: http://dx.doi.org/10.15666/aeer/2202_16671682

[6] Han, H. K., Miao, J. Y., Zhang, Y. Y., Zhang, D. Z., Zong, G. H., Gong, X. W., Li, J., Feng, B. L. (2018): Estimating chlorophyll content of proso millet canopy by hyperspectral reflectance. – Agricultural Research in the Arid Areas 36(1): 164-170.
[7] He, J., Liu, B. F., Li, S. M., Guo, Y., Wang, L. G., Zhang, Y., Li, J. (2017): Winter wheat grain protein content monitoring model driven by hyperspectral remote sensing images at different growth stages. – Chinese Journal of Eco-Agriculture 25(6): 865-875.
[8] Li, X., Zhao, S. W., Bao, X. X., Wu, Y. J., Yang, Z. C. (2024): Effects of photoperiods on morphology, photosynthetic characters and carbohydrate of cucumber seedlings. – Journal of China Agricultural University 29(04): 164-172.
[9] Li, Z. H., Yang, G. J., Wang, J. H., Xu, X. G., Song, X. Y. (2018): Remote sensing of grain protein content in cereal: a review. – China Agricultural Informatics 30(1): 46-54.
[10] Liu, C., Peng, Y., Fang, S. H. (2020): Remote estimation of rice leaf net photosynthetic rate based on hyperspectral reflectance. – Journal of China Agricultural University 25(01): 56-65.
[11] Liu, T., Wu, H. W., Cao, Z. (2016): Prediction model on net photosynthetic rate of rice based on support vector machine. – Journal of Chinese Agricultural Mechanization 37(09): 151-153.
[12] Lv, W., Li, Y. H., Mao, W. B., Gong, X., Chen, S. G. (2017): Comparison of estimation methods for net photosynthetic rate of wheat's flag leaves based on hyperspectrum. – Journal of Agricultural Resources and Environment 34(06): 582-586.
[13] Miao, M. K., Wang, B. S., Li, C. C., Long, H. L., Yang, G. J., Feng, H. K., Zhai, L. T., Liu, M. X., Wu, Z. C. (2020): Remote sensing estimation of maximum net photosynthetic rate of winter wheat leaves based on continuous wavelet transform. – Jiangsu Journal of Agricultural Sciences 36(03): 544-552.
[14] Qiao, Y. Y., Zhao, W. Q., Hu, X. Z., Li, X. P. (2016): Determination of protein content in oat using near-infrared spectroscopy. – Journal of the Chinese Cereals and Oils Association 31(8): 138-142.
[15] Qu, S., Li, Z. H., Qiu, C. X., Yang, G. J., Song, X. Y., Chen, Z. X., Liu, C. (2017): Remote sensing prediction of winter wheat grain protein content based on nitrogen nutrition index at anthesis stage. – Transactions of the Chinese Society of Agricultural Engineering 33(12): 186-193.
[16] Ran, W. L., Guo, J. M., Ma, Y., Mao, J., Han, X. P., Zheng, B. Y., Li, D. L., Shao, R. X., Yang, Q. H. (2017): Effect of supplemental lumination at night on endogenous plant hormones content and photosynthetic characteristics in wheat leaves. – Journal of Triticeae Crops 37(09): 1181-1186.
[17] Shen, Y. Z., Guo, S. S. (2015): Effect of photoperiod on growth, development, yield and nutritional quality of wheat in controlled system. – Journal of Triticeae Crops 35(01): 64-70.
[18] Sheng, Y. Y., Xu, X. M., Zhang, Q. H., Zhang, L. X. (2022): Advances in synthetic biology for photosynthetic carbon assimilation. – Synthetic Biology Journal 3(05): 870-883.
[19] Singh, T., Garg, N. M., Iyengar, S. R. S. Singh, V. (2023): Near-infrared hyperspectral imaging for determination of protein content in barley samples using convolutional neural network. – Journal of Food Measurement and Characterization 17(4): 3548-3560.
[20] Sonobe Rei, Hirono Yuhei, Oi Ayaka. (2020): Non-destructive detection of tea leaf chlorophyll content using hyperspectral reflectance and machine learning algorithms. – Plants 9(3): 368-368.
[21] Tian, C. Y., Huang, C. Y., Guo, X. F., Liu, X. Y., Wang, D. W. (2018): Correlation analysis between cotton canopy reflectance spectra and leaf net photosynthetic rate. – Remote Sensing Information 33(01): 99-103.
[22] Tian, G., Liu, X., Li, H. X., Wang, Y. W., Liu, Y. Z., Li, W. X., Cao, J. J., Cheng, K., Wang, Z. H., Liu, H. (2021): Correlation analysis between distribution of dry matter in

http://www.aloki.hu ● ISSN 1589 1623 (Print) ● ISSN 1785 0037 (Online)
DOI: http://dx.doi.org/10.15666/aeer/2202_16671682

various organs and grain yield in different varieties of foxtail millet. – Molecular Plant Breeding 19(01): 240-247.

[23] Tian, X., Qin, H. B., Wang, J. J., Qiao, Z. J. (2021): Rapid determination of millet quality by near infrared reflectance spectrometry. – Cereals & Oils 34(10): 145-148.

[24] Vohland, M., Besold, J., Hill, J., Fründ, H. C. (2011): Comparing different multivariate calibration methods for the determination of soil organic carbon pools visible to near infrared spectroscopy. – Geoderma 166: 198-205.

[25] Wang, J. J., Chen, L., Wang, H. G., Cao, X. N., Liu, S. C., Tian, X., Qin, H. B., Qiao, Z. J. (2019): Effects of hyperspectral prediction on leaf nitrogen content and the grain protein content of broomcorn millet. – Scientia Agricultura Sinica 52(15): 2593-2603.

[26] Wang, J. J., Tian, X., Qin, H. B., Wang, H. G., Cao, X. N., Chen, L., Liu, S. C., Qiao, Z. J. (2021): Regulation effects of photoperiod on growth and leaf endogenous hormones in broomcorn millet. – Scientia Agricultura Sinica 54(02): 286-295.

[27] Wang, Q. (2022): Effects of low-light stress on grain formation and yield of different maize genotypes. – Northwest A&F University.

[28] Wang, Y., Xu, S. T., Yao, H. Y., Yang, K. J., Li, Y. H. (2020): Retrieval of flag leaf net photosynthetic rate of wheat using hyperspectral remote sensing based on wavelet transform. – Journal of Zhejiang Agricultural Sciences 61(10): 1070-1984.

[29] Yang, H. J., Yuan, X. Y., Qi, X., Guo, P. Y., Guo, D. X., Dong, S. Q., Wen, Y. Y., Zhang, L. G. (2017): Photosynthetic physiological response of foxtail millet to weak light stress at jointing-stage. – Journal of Nuclear Agricultural Science 31(02): 386-393.

[30] Zhang, C., Liu, F., Kong, W. W., He, Y. (2015): Application of visible and near-infrared hyperspectral imaging to determine soluble protein content in oilseed rape leaves. – Sensors 15(7).

[31] Zhang, S., Feng, M. C., Yang, W. D., Wang, C., Sun, H., Jia, X. Q., Wu, G. H. (2018): Detection of grain content in winter wheat based on near infrared spectroscopy. – Chinese Journal of Ecology 37(4): 1276-1281.

[32] Zhang, X. M., Hou, X. X., Su, Y. M., Yan, X. B., Qiao, X. X., Yang, W. D., Feng, M. C., Kong, H. H., Zhang, Z., Shafiq Fahad, Han, W. J., Li, G. X., Chen, P., Wang, C. (2023): Analyzing protein concentration from intact wheat caryopsis using hyperspectral reflectance. – Chemical and Biological Technologies in Agriculture 10(1): 83.

[33] Zhao, L. H., Gong, Y. Y., Zhang, J., Lin, C. B., Wang, Y., Li, X. W., Dai, X., Jiang, Y. (2020): Rapid determination of quinoa seeds crude protein content using near infrared spectroscopy. – Science and Technology of Food Industry 41(15): 233-236 + 243.

http://www.aloki.hu ● ISSN 1589 1623 (Print) ● ISSN 1785 0037 (Online)
DOI: http://dx.doi.org/10.15666/aeer/2202_16671682